Inorganic Chemistry

Article

pubs.acs.org/IC

Hydroxypyridinonate Complex Stability of Group (IV) Metals and Tetravalent f-Block Elements: The Key to the Next Generation of Chelating Agents for Radiopharmaceuticals

Manuel Sturzbecher-Hoehne, Taylor A. Choi, and Rebecca J. Abergel*

Chemical Sciences Division, Lawrence Berkeley National Laboratory, Berkeley, California 94720, United States

Supporting Information

ABSTRACT: The solution thermodynamics of the water-soluble complexes formed between 3,4,3-LI(1,2-HOPO) and Zr(IV) or Pu(IV) were investigated to establish the metal coordination properties of this octadentate chelating agent. Stability constants log β_{110} = 43.1 ± 0.6 and 43.5 ± 0.7 were determined for [Zr(IV)(3,4,3-LI(1,2-HOPO))] and [Pu(IV)(3,4,3-LI(1,2-HOPO))], respectively, by spectrophotometric competition titrations against Ce(IV). Such high thermodynamic stabilities not only confirm the unparalleled Pu(IV) affinity of 3,4,3-LI(1,2-HOPO) as a decorporation agent but also corroborate the great potential of hydroxypyridinonate ligands as new ^{89}Zr-chelating platforms for immuno-PET applications. These experimental values are in excellent agreement with previous estimates and are discussed with respect to ionic radius and electronic configuration, in comparison with those of Ce(IV) and Th(IV). Furthermore, a liquid chromatography assay combined with mass spectrometric detection was developed to probe the separation of the neutral [M(IV)(3,4,3-LI(1,2-HOPO))] complex species (M = Zr, Ce, Th, and Pu), providing additional insight into the coordination differences between group IV and tetravalent f-block metals and on the role of d and f orbitals in bonding interactions.

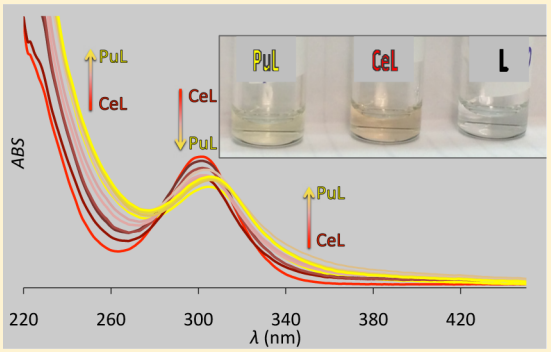

INTRODUCTION

The radiometal zirconium-89 (^{89}Zr) has recently emerged as an ideal positron emitter for the design and synthesis of radioimmunoconjugates in positron emission tomography (PET) imaging applications[1,2] because the relatively long half-life of ^{89}Zr ($t_{1/2}$ = 78.4 h) is compatible with the use of monoclonal antibodies (mAbs) that possess long biological half-lives (typically, 2−4 days), and this approach represents the most rapidly expanding category of therapeutics.[3−5] The common strategy for labeling mAbs with metallic radioisotopes utilizes bifunctional chelating agents that are easily conjugated to a targeting antibody,[2] such as derivatives of the well-known chelators ethylenediaminetetraacetic acid (EDTA), diethylenetriaminepentaacetic acid (DTPA), and 1,4,7,10-tetraazacyclododecane-1,4,7,10-tetraacetic acid (DOTA) or the natural siderophore, desferrioxamine (DFO, Figure 1).[2,6] However, while Zr^{4+} has been shown to form thermodynamically stable octadentate dodecahedral complexes with DTPA, EDTA, and DOTA, these complexes are not suitable for use *in vivo* due to their poor kinetic stability.[7−10] The hexadentate ligand DFO that contains three hydroxamate metal-binding moieties is, to date, the only ligand successfully used in preclinical and clinical ^{89}Zr-immuno-PET studies.[11−13] Nevertheless, recent preclinical studies using ^{89}Zr-DFO-labeled tracers have called attention to moderate levels of ^{89}Zr uptake in the bone (up to 15% of the injected dose), most likely as a result of the release of Zr^{4+} from the administered chelate, thereby highlighting the need for new stable ^{89}Zr chelators.[1,2,14,15] The small ionic radius and high charge of Zr^{4+}, the predominant ion in aqueous solution, make it a hard Lewis acid with high affinities for oxygen-containing donor ligands, similarly to the f-block metal ions Ce^{4+}, Th^{4+}, and Pu^{4+}.[16−18] Over the past 2 decades, multidentate hydroxypyridinonate (HOPO) ligands have been extensively studied for their outstanding abilities to scavenge lanthanide and actinide ions and may therefore constitute ligands of choice for Zr^{4+} chelation.[19] The octadentate ligand 3,4,3-LI(1,2-HOPO) (Figure 1) is currently undergoing development as a prospective therapeutic for the treatment of individuals contaminated with selected threat actinides (U, Np, Pu, Am, and Cm),[20,21] and it received an Investigational New Drug designation from the U.S. Food and Drug Administration in 2014 based on a number of *in vivo* experimental studies establishing its low toxicity and unparalleled actinide decorporation efficacy.[22−25] In addition, the *in vivo* stability of the [Pu(IV)(3,4,3-LI(1,2-HOPO))] complex has been demonstrated in mice,[25] leading to quantitative elimination of the administered complex within 24 h with no residual contaminant. Recent studies have also suggested that 3,4,3-LI(1,2-HOPO) may be radiolabeled with ^{89}Zr using standard rapid procedures adequate for clinical settings and have started

Received: January 6, 2015
Published: March 23, 2015

DOI: 10.1021/acs.inorgchem.5b00033
Inorg. Chem. 2015, 54, 3462−3468

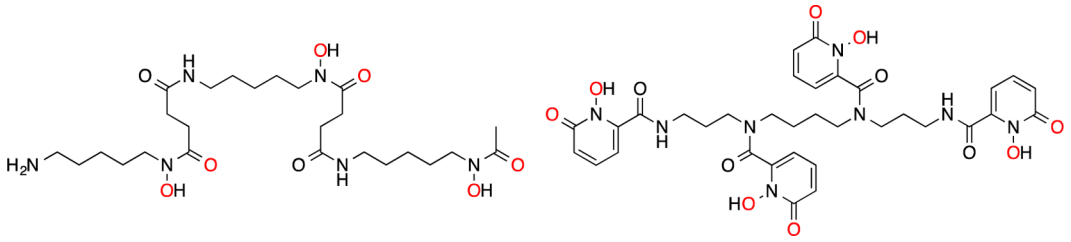

Figure 1. Structures of DFO (left) and 3,4,3-LI(1,2-HOPO) (right); metal-binding atoms are shown in red.

exploring the *in vitro* and *in vivo* properties of the resulting complex.[14] Importantly, high *in vivo* stability was observed in those initial biodistribution studies, thus suggesting that 3,4,3-LI(1,2-HOPO) is a promising new synthetic platform for the development of ^{89}Zr-immuno-PET tracers. However, while *in vitro* stability behavior was evaluated through computational methods and transchelation challenge experiments, the thermodynamic parameters of complexation were not determined. The initial purpose of the work reported here was, therefore, to rigorously characterize the solution thermodynamic stability of the Zr(IV) complex formed with 3,4,3-LI(1,2-HOPO), supporting further development of this ligand as a ^{89}Zr radiopharmaceutical. In addition, to complement previous work on *in vivo* actinide sequestration and *in vitro* solution characterization of lanthanide and early actinide complexes, this thermodynamic characterization was extended to the complexation of Pu(IV), providing a series of comparative data sets to evaluate the coordination similarities of group IV metals and tetravalent f-block ions.

EXPERIMENTAL SECTION

Caution: *^{232}Th and ^{242}Pu are radionuclides that should be manipulated only in a specifically designated facility in accordance with appropriate safety controls. All spectroscopic measurements were undertaken either in controlled facilities and/or using multiple containment procedures.*

General Considerations. Chemicals were obtained from commercial suppliers and were used as received. The ligand 3,4,3-LI(1,2-HOPO) was prepared and characterized as previously described.[20] 99.99% $ZrCl_4$ stored in an ampule was purchased from Sigma-Aldrich. Solutions of Ce(IV) and Th(IV) were prepared from $Ce(SO_4)_2{\cdot}4H_2O$ and $^{232}ThCl_4{\cdot}8H_2O$ (Baker & Adamson, ACS grade), respectively. The ^{242}Pu was received from Oak Ridge National Laboratory as PuO_2 (lot Pu-242-327 A, 99.93 wt % of metal ^{242}Pu), and a stock solution of Pu(IV) was prepared as described previously.[26] All solutions were prepared using deionized water purified by a Millipore Milli-Q reverse osmosis cartridge system, and special care was taken to adjust the pH with concentrated HCl, H_2SO_4, or NaOH when needed. All thermodynamic measurements were conducted at room temperature (unless otherwise indicated).

Ligand and Metals Stock Solutions. Aqueous stock solutions of 3,4,3-LI(1,2-HOPO) were freshly prepared by direct dissolution of a weighed portion of ligand in water prior to each set of experiments. A stock solution of Ce(IV) was made in 3.0 M H_2SO_4, and the presence of Ce(III) was determined using fluorescence spectroscopy, as previously described.[27] A Zr(IV) stock solution was prepared by dissolving $ZrCl_4$ in 3.0 M H_2SO_4 to prevent hydrolysis. The metal salt $ZrCl_4$ was handled and stored in a glovebox kept under an inert atmosphere. The Zr(IV) stock solution was standardized against EDTA, with xylene orange as the indicator.[28] A 2 mM ^{242}Pu(IV) working stock solution in 1.25 M H_2SO_4 was prepared from a solution of 100 mM ^{242}Pu(IV) in 4 M HNO_4. The 100 mM ^{242}Pu stock was evaluated by UV/vis, and a purity of 99.9% was established by gamma spectroscopy. A Th(IV) stock solution was prepared in 0.1 M H_2SO_4.

Metal Competition Batch Titrations. The experimental setup for these titrations is similar to that of previously described systems.[27] Varying amounts of competing metal (M_{comp}(IV): Zr(IV) or Pu(IV)) were added to solutions assembled from stocks of 3,4,3-LI(1,2-HOPO), a measured aliquot of the Ce(IV) stock solution, and the supporting electrolyte solution (3.0 M Na_2SO_4), with resulting ligand and Ce(IV) concentrations of 50 μM and the ratio [M_{comp}(IV)]/[Ce(IV)] between 0 and 2. Four series of titrations were performed for each competing metal, with different concentrations of H_2SO_4 (0.125, 0.25, 0.5, and 1 M), to prevent the formation of hydrolysis products as well as the reduction of Ce(IV) and to control the pH. Each titration was performed independently at least two times and included 22 data points. All samples were equilibrated for 72 h at room temperature before pH and UV−vis measurements (230−700 nm).

pH Measurements. The pH of each injected solution was measured with a conventional pH meter at 25 °C (713 pH meter, Metrohm Brinkmann) that was equipped with a glass electrode (Micro Combi Electrode, Metrohm) filled with KCl and calibrated with pH standards before each titration.

UV−Visible Spectroscopy. Absorption spectra were recorded on a Varian Cary G5 double-beam absorption spectrometer or a NanoDrop 2000C, using quartz cells of 10 and 2 mm path lengths, respectively.

Fluorescence Spectroscopy. Fluorescence spectra were acquired on a HORIBA Jobin Yvon IBH FluoroLog-3 spectrofluorimeter used in steady-state mode. A continuous xenon lamp (450 W) was used as the light source. Spectral selection was achieved by passage through a double grating excitation monochromator (2.1 nm/mm dispersion, 1200 grooves/mm). Emission was monitored perpendicular to the excitation, again with spectral selection achieved by passage through a double grating excitation monochromator (2.1 nm/mm dispersion, 1200 grooves/mm). A thermoelectrically cooled single-photon detection module (HORIBA Jobin Yvon IBH, TBX-04-D) was used as the detector. Signals were acquired using an IBH DataStation Hub photon counting module.

Data Treatment. The stability constants and spectral deconvolution were refined using the least-squares fitting program HypSpec.[29,30] Examples of fits are provided in Figures S1 and S2 of the Supporting Information. All equilibrium constants were defined as cumulative formation constants, β_{mlh}, according to eq 1, where the metal and ligand are designated M and L, respectively. All metal and ligand concentrations were held at estimated values determined from the volume of standardized stock solutions. All species formed with ligands L were considered to have significant absorbance observed in the UV−vis spectra and were therefore included in the refinement process. The refinements of the overall formation constants β included, in each case, previously determined ligand protonation constants[31,32] and the metal hydrolysis products, whose equilibrium constants were fixed to the literature values.[33] The pM values were calculated using the modeling program Hyss.[34,35] Errors were determined as $t^*s/(n)^{1/2}$ at the 95% probability level, where n is the number of samples, $s/(n)^{1/2}$ is the standard deviation, and t^* is the distribution over $n - 1$ degrees of freedom. These errors were used in the variance formula to account for error propagation.

$$mM + lL + hH \leftrightarrow [M_mL_lH_h];\ \beta_{mlh} = \frac{[M_mL_lH_h]}{[M]^m[L]^l[H]^h} \quad (1)$$

DOI: 10.1021/acs.inorgchem.5b00033
Inorg. Chem. 2015, 54, 3462−3468

Mass Spectrometry: Direct Injection. Mass spectra after direct sample infusion were obtained on a 6120 Quadrupole MS (Agilent Technologies, Santa Clara, CA, USA) equipped with an electrospray ionization source. For direct injections, a syringe pump (KD Scientific, Holliston, MA, USA) delivered the samples to the mass spectrometer with a constant flow rate of 100 μL/min. The voltage applied to the capillary was 3.5 and 3.2 kV in the positive and negative detection modes, respectively. A nitrogen gas flow rate of 12 L/min was used to assist the nebulization process. The cone voltage was set to 100 V in positive mode and 50 V in negative mode, and the ion source temperature was 300 °C. Mass spectra were recorded over a 100−1000 m/z range over collection times of 1 min. Solutions of 3,4,3-LI(1,2-HOPO), [Ce(IV)(3,4,3-LI(1,2-HOPO))], and [Zr(IV)(3,4,3-LI(1,2-HOPO))] were injected at a concentration of 50 μM. 3,4,3-LI(1,2-HOPO) stock was diluted in H_2O with a final pH of 3.6, whereas the metal−ligand complexes were prepared from 3,4,3-LI(1,2-HOPO) and metal stock solutions, with a final pH of 1.5.

Liquid Chromatography−Mass Spectrometry Assay. Aqueous solutions of 3,4,3-LI(1,2-HOPO), [Ce(IV)(3,4,3-LI(1,2-HOPO))], [Zr(IV)(3,4,3-LI(1,2-HOPO))], [^{232}Th(IV)(3,4,3-LI(1,2-HOPO))], and [^{242}Pu(IV)(3,4,3-LI(1,2-HOPO))] were prepared from 3,4,3-LI(1,2-HOPO) and metal stock solutions in 0.5% formic acid at respective concentrations of 25, 0.25, 0.25, 0.25, and 1 μM, with a final pH of 2.2. Samples were assayed in duplicate on a UPLC Waters Xevo system interfaced to a QTOF mass spectrometer (Waters Corporation, Milford, MA, USA) in Micromass Z-spray geometry. Chromatographic separation was achieved on an analytical Zorbax Eclipse column (Agilent Technologies, XDB-C18, 5 μm, 4.6 × 150 mm or XDB-C8, 5 μm, 4.6 × 150 mm) maintained at ambient temperature with two 0.5% formic acid mobile phases [(A) in water and (B) in methanol]. Samples (10 μL) were eluted using a gradient initially held constant at 7% B for 6.0 min and were then progressed to 40% B in the next 6.0 min and held at 40% B for 10 min. Mobile phase B was then increased to 99% over 3.0 min, held constant at 99% for 5.0 min, and then rapidly switched to 7% B and held until 46 min for equilibration. The flow rate was maintained at 0.5 mL/min. The mass spectrometer equipped with an ESI source was operated in positive ion mode, and mass spectra were acquired in the continuum mode across the m/z range of 100−1200, at 5 s per scan, with a 14 ms interscan delay. Data acquisition and instrument control were accomplished using MassLynx software, version 4.1. Samples were infused into the ionization chamber from the LC system. The operating parameters were as follows: the nebulization gas flow rate was set to 600 L/h with a desolvation temperature of 375 °C, the cone gas flow rate was set to 30 L/h, and the ion source temperature was 125 °C. The capillary, sampling cone, and extraction cone voltages were tuned to 2.7 kV, 47 V, and 3.3 V, respectively. Liquid nitrogen served as nebulizer and argon was used as collision gas with collision energies up to 50 eV. A calibration check of the instrument was performed daily with 0.5 mM sodium formate, prior to sample analysis.

RESULTS AND DISCUSSION

[M(IV)(3,4,3-LI(1,2-HOPO))] Solution Stability Determination (M = Zr, Pu). Similarly to that for Ce^{4+} and Th^{4+}, the aqueous solution chemistry of Zr^{4+} and Pu^{4+} can be difficult to characterize due to the formation of hydrolysis products and oligomers of the metal ions.[33,36−38] In addition, direct spectroscopic titration methods are not suitable to follow the appearance of very strong complexes such as those formed with the HOPO ligands. However, indirect spectrophotometric competition titrations methods can be applied between metal ions with similar thermodynamic affinities for a specific ligand[27] and were used for the stability determination of [Zr(IV)(3,4,3-LI(1,2-HOPO))] and [Pu(IV)(3,4,3-LI(1,2-HOPO))], using Ce(IV) as a competing metal. Figure 2 reflects the changes in UV−vis absorbance upon the addition of 0−2 equiv of Zr(IV) or Pu(IV) to a solution of [Ce(IV)(3,4,3-LI(1,2-HOPO))]. In the Zr(IV) titration, the sharp band characteristic of the 1,2-HOPO residues underwent a red shift from 301 to 305 nm, most likely because of the lesser acidity of Zr(IV) compared to that of Ce(IV), which decreases the absorbance energy of the aromatic 1,2-HOPO rings, with an isosbestic point at 264 nm. Simultaneously, the large ligand-to-metal charge transfer (LMCT) band centered at 450 nm characteristic of [Ce(IV)-(3,4,3-LI(1,2-HOPO))] slowly disappeared. In the Pu(IV) titration, a larger red shift is observed from 301 to 310 nm, with an isosbestic point at 280 nm. In addition, a new LMCT band centered at 390 nm appears with the formation of [Pu(IV)-(3,4,3-LI(1,2-HOPO))]. The competition titrations were performed in sulfuric media (Na_2SO_4, I = 3.0 M) at high proton concentrations (0.125 to 1 M H_2SO_4) to prevent hydrolysis of the metal ions and to avoid the reduction of Ce(IV) after its release by the ligand. No proton dependency was observed for the Zr(IV) and Pu(IV) complex stability constants (Figure S3, Supporting Information), indicating that only two complex species (one per metal) were involved in the competition equilibrium over the examined acidic pH range. The stability constant for [Ce(IV)(3,4,3-LI(1,2-HOPO))] (log β_{110} = 41.5) was previously determined at 0.4 M ionic strength.[27] The specific ion interaction theory (SIT) was

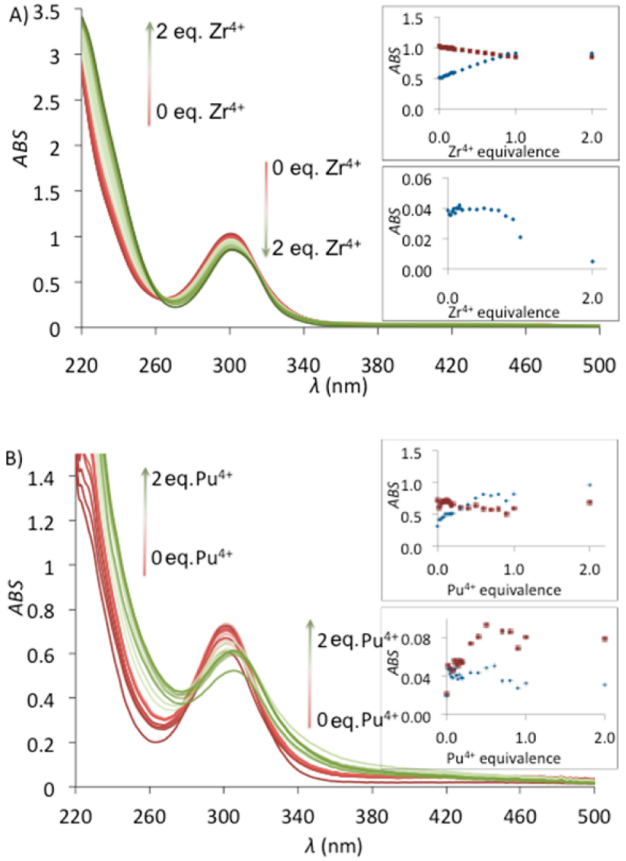

Figure 2. (A) Metal competition batch titration of [Ce(IV)(3,4,3-LI(1,2-HOPO))] against Zr(IV). [Ce] = [3,4,3-LI(1,2-HOPO)] = 50 μM, [Zr]/[Ce] = 0−2, [H_2SO_4] = 0.5 M, pH 1.3, I = 3.0 M (Na_2SO_4), T = 20 °C, l = 10 mm. Insets: Change in absorbance at 250 nm (top, blue), 300 nm (top, red), and 430 nm (bottom, blue) versus equivalents of Zr(IV). (B) Metal competition batch titration of [Ce(IV)(3,4,3-LI(1,2-HOPO))] against Pu(IV). [Ce] = [3,4,3-LI(1,2-HOPO)] = 180 μM, [Pu]/[Ce] = 0−2, [H_2SO_4] = 0.5 M, pH 1.3, I = 3.0 M (Na_2SO_4), T = 20 °C, l = 2 mm. Insets: Change in absorbance at 250 nm (top, blue), 300 nm (top, red), 370 (bottom, red), and 450 nm (bottom, blue) versus equivalents of Pu(IV).

DOI: 10.1021/acs.inorgchem.5b00033
Inorg. Chem. 2015, 54, 3462−3468

Table 1. Summary of the Thermodynamic and Chromatographic Parameters Determined for [M(IV)(3,4,3-LI(1,2-HOPO))] Complexes (M = Zr, Ce, Th, Pu) and Comparison with Corresponding DTPA Complexes

	3,4,3-LI(1,2-HOPO)		DTPA		3,4,3-LI(1,2-HOPO)		
cation	log β_{110}	pM[a]	log β_{110}	pM[a]	C8 rel. ret. time (min)	C18 rel. ret. time (min)	metal ionic radius (pm, CN = 8)[51]
Zr^{4+}	43.1(6)	44.0(6)	35.8	33.9	1.13	1.15	84
Ce^{4+}	41.5(5)	42.4(5)	34.0	30.6	1.23	1.26	97
Th^{4+}	40.1(5)	41.0(5)	28.7	26.8	1.26	1.31	105
Pu^{4+}	43.5(7)	44.5(7)	33.7	31.7	1.24	1.29	96

[a]pM is the negative logarithm of the free metal concentration in equilibrium with complexed and free ligand at a fixed pH (pH 7.4 for physiological conditions) with 1 μM total metal concentration and 10 μM total ligand concentration. Hydrolysis constants of cations were set to the values found in the NIST database[33] at the lowest ionic strength available; pK_a values for 3,4,3-LI(1,2-HOPO) were set to 3.87, 5.01, 5.68, and 6.64;[31] pK_a values for DTPA were set to 1.5, 2.64, 4.27, 8.60, and 10.58.[55]

therefore applied here to correct for the experimental differences in ionic strength, using established SIT parameters for Th(IV) with SO_4^{2-}, since such parameters have not yet been determined for Zr(IV), Pu(IV), or Ce(IV) in sulfate media.[39] A corrected log β_{110} value of 40.0 for [Ce(IV)(3,4,3-LI(1,2-HOPO))] at I = 3.0 M was used for the deconvolution and least-squares refinements of the spectral data from the Ce(IV)/Zr(IV) and Ce(IV)/Pu(IV) competitions. For an average ionic strength of 0.4 M, the final stability constants for the Zr(IV) and Pu(IV) complexes were then determined as log β_{110} (Zr^{IV}) = 43.1 ± 0.6 and log β_{110} (Pu^{IV}) = 43.5 ± 0.7, corresponding to respective conditional pM values of 44.0 ± 0.6 and 44.5 ± 0.7 (Table 1), where the pM value is defined as the negative logarithm of the free metal concentration in equilibrium with complexed and free ligand at a fixed pH of 7.4 (for physiological conditions) and for fixed ligand and metal concentrations of 10 and 1 μM, respectively. Calculation of this pM parameter provides a convenient way to compare ligands of varying acidity and/or denticity, especially for discussions relevant to physiological conditions and biological applications. The calculated speciation diagrams (Figure 3), with fixed concentrations of metal (1 μM, M = Zr, Pu, or Th) and ligand (10 μM), indicate that the main species found in solution at pH 7.4 are the [M(IV)(3,4,3-LI(1,2-HOPO))] complexes, with the first appearance of hydroxide species occurring under very basic conditions (for minimum pH values of 10). In addition, determination of the pM value as a function of pH highlights the formation of these extremely stable Zr(IV), Ce(IV), Th(IV), and Pu(IV) complexes over a large pH range (Figure 3).

Not only are the Zr(IV) and Pu(IV) stability constants the highest ever reported for metal complexes of 3,4,3-LI(1,2-HOPO) but also they are the highest known for Zr(IV) or Pu(IV) complexes in aqueous solution. Mostly for historical reasons, *in vivo* studies assessing the radionuclide decorporation efficacy of 3,4,3-LI(1,2-HOPO) have often, if not always, included DTPA as a decorporation reference and demonstrated drastically improved radionuclide removal from contaminated bodies when using the experimental HOPO ligand.[20,22,24] The *in vitro* thermodynamic stability of the Pu(IV) complex formed with 3,4,3-LI(1,2-HOPO) was determined here as being up to 13 orders of magnitude higher than that of the DTPA complex (log β_{110} (Pu^{IV}) = 33.7[16] or 29.5,[33] corresponding to a calculated pM = 31.7 or 31.5, respectively), correlating with the highest *in vivo* Pu decorporation efficacy reported to date.[20,40] Similarly, in comparison to the stability of complexes formed with DFO, DTPA, or citrate, the standard chelators encountered in ^{89}Zr imaging studies, the stability of [Zr(IV)-(3,4,3-LI(1,2-HOPO))] is increased by at least 9 orders of magnitude. Surprisingly, the solution thermodynamic stability of DFO with Zr(IV) has never been characterized, and the corresponding constants are unknown.[41,42] However, based on previous results and comparison with Th(IV), a pM between 29 and 31 can be estimated for the Zr(IV) complex of DFO.[27] This value is slightly higher than that of the Zr(IV) citrate complex, 28.7,[33,41] but it is still lower than that of the DTPA complex, calculated at 35.0.[27,33,43,44] It is noteworthy that radiopharmaceutical applications of 3,4,3-LI(1,2-HOPO) are not limited to ^{89}Zr-immunoconjugates. Over the past few years, new developments in the use of radionuclides for immunotherapy have highlighted the tremendous potential of targeted alpha therapy using short-lived alpha-particle emitters such as

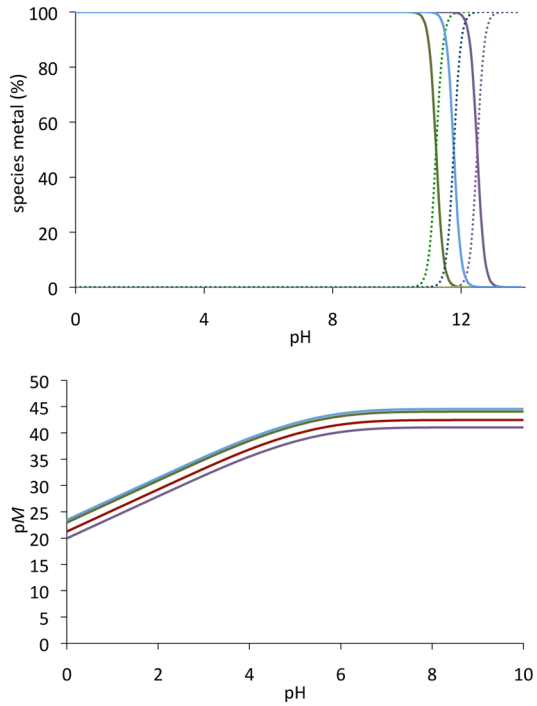

Figure 3. (Top) Calculated speciation diagram for the complexation of M(IV) by 3,4,3-LI(1,2-HOPO) (M = Zr (green), Pu (blue), or Th (purple)) at fixed concentrations of 1 μM metal, 10 μM ligand, and 0.4 M ionic strength. The complexed species [M(IV)(3,4,3-LI(1,2-HOPO))] are shown as solid lines, and the hydroxide species $M(IV)(OH)_4$, as dotted lines. Hydrolysis constants of M(IV) were set to the values found in the NIST database at the lowest ionic strength available; pK_a values for 3,4,3-LI(1,2-HOPO) were set to 3.87, 5.01, 5.68, and 6.64. (Bottom) pM(M^{IV}) values as functions of pH for [M(IV))(3,4,3-LI(1,2-HOPO))] complexes (M = Zr (green), Ce (red), Th (purple), and Pu (blue)).

DOI: 10.1021/acs.inorgchem.5b00033
Inorg. Chem. 2015, 54, 3462−3468

^{227}Th ($t_{1/2}$ = 18.7 days).[45] However, strategies of alpha-emitter delivery to target sites through immunoconjugates present similar challenges as those encountered for other radiometals such as ^{89}Zr: available chelating agents lack thermodynamic affinity and/or fast kinetics of complexation.[46,47] Recently, Pham et al. reported a new macrocyclic octadentate therephthalamide (TAM) chelator, with presumed unprecedented affinity for Th^{4+}.[46] Nevertheless, despite extremely high complex formation constants, a pM(Th(IV)) value of 39.1 was determined for this ligand at physiological pH, which is still 2 orders of magnitude lower than that for 3,4,3-LI(1,2-HOPO).[27] Although both 1,2-HOPO and TAM metal-binding units are extremely effective at binding Th(IV), TAM units are more basic and are therefore less efficient at physiological pH but more efficient under basic conditions (pH 9). The overall ligand basicity can be quantified from the sum of the log K_a values associated with only those four protonation steps that affect metal binding, with $\sum$ log K_a = 21.2 for 3,4,3-LI(1,2-HOPO)[31] and $\sum$ log K_a = 23.4 for the TAM ligand.[46] In this particular case, the higher acidity of 3,4,3-LI(1,2-HOPO) makes it a unique versatile ligand for Th(IV).

[M(IV)(3,4,3-LI(1,2-HOPO))] Mass Spectrometry and Liquid Chromatography (M = Zr, Ce, Th, Pu). To confirm the successful competition with hydrolysis products and quantitative *in situ* formation of 3,4,3-LI(1,2-HOPO) complexes, even at low pH values, Ce(IV) and Zr(IV) complex aqueous solutions were first analyzed by mass spectrometry through direct infusion. The mass analysis in positive mode of the free ligand and the corresponding Ce(IV) and Zr(IV) complexes is depicted in Figure S4 (Supporting Information) and supports the high stability constants. For [Ce(IV)(3,4,3-LI(1,2-HOPO))], singly and doubly charged species were observed at 887 and 444 *m/z*, respectively, similar to what was observed for [Zr(IV)(3,4,3-LI(1,2-HOPO))], with major peaks at 837 and 419 *m/z*. The ligand itself forms additional sodium adducts with major signals at 751 and 773 *m/z* for singly charged species and 376, 387, and 398 *m/z* for doubly charged species. While 3,4,3-LI(1,2-HOPO) also yielded signals in negative mode with 749 and 374 *m/z*, the neutral metal complexes could not be detected due to the lack of formation of negative ions. No hydrolysis product was observed in the mass spectra. Metal complex aqueous solutions (M = Zr, Ce, Th, and Pu) were then prepared in 0.5% formic acid and analyzed by liquid chromatography combined with mass spectrometry in positive ion mode. A relatively high concentration of free ligand (25 μM) was first injected into the system to obtain a good chromatogram. This first injection was also used to flush the column and to ensure the removal of all interfering trace metal ions. The Zr(IV), Ce(IV), and Th(IV) complexes were introduced at 250 nM onto the column, and sufficient ion counts were detected in the ionization process. However, a higher concentration of the Pu(IV) complex (1000 nM) was introduced due to an insufficient number of ions formed at lower concentrations (resulting in ion counts at least 2-fold higher than that for the Zr(IV) and Ce(IV) complexes). The primary stock of ^{242}Pu used in this study was originally prepared in 4 M HNO_3, and, despite large dilutions (>500-fold), nitrate traces likely resulted in ion suppression. The chromatograms showed well-separated single peaks, reflecting the quantitative single complex species formation (Figure 4). For all four metal complexes, singly charged species were detected, corresponding to the protonated cations $[M(IV)LH]^+$ and the sodium, $[M(IV)LNa]^+$, and potassium, $[M(IV)LK]^+$, adducts, with the Na adducts yielding the predominant peaks. The assay was applied to two reverse-phase analytical columns, containing octyl (C8) or octadecyl (C18) silica-bonded materials. Sharper peaks were obtained using the less hydrophobic C8 column, but a slightly better separation of the peaks corresponding to the different ligand and metal species was observed with the C18 column. In both cases, retention times increased from the ligand to the metal species and in the following order for the different [M(IV)-(3,4,3-LI(1,2-HOPO))] complexes: Zr < Ce < Pu < Th; this is indicative of decreasing polarity.

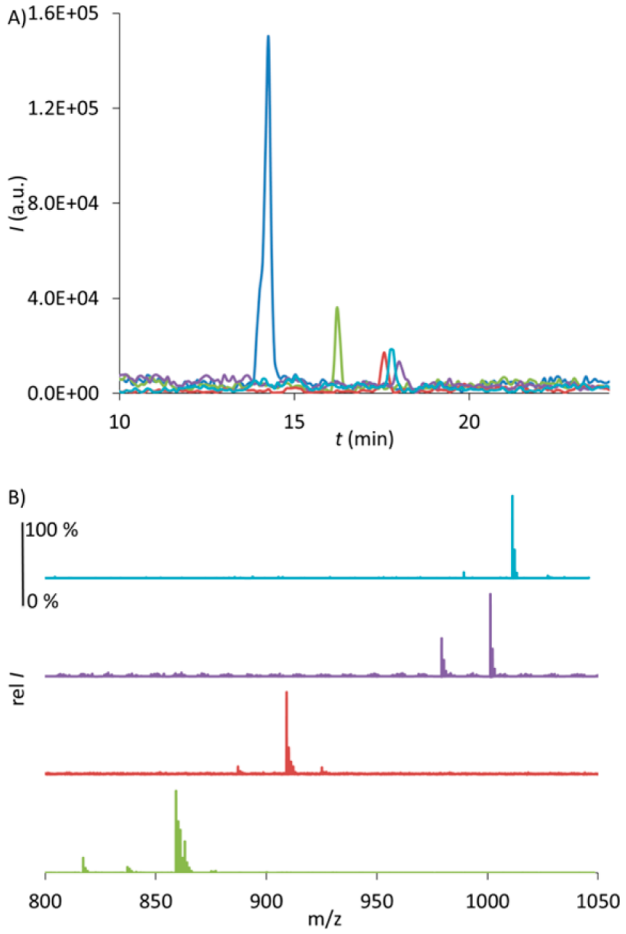

Figure 4. (A) Overlay of liquid chromatograms of free 3,4,3-LI(1,2-HOPO) (dark blue) and [M(IV))(3,4,3-LI(1,2-HOPO))] complexes (M = Zr (green), Ce (red), Th (purple), Pu (light blue)) obtained with the C8 column. (B) Mass analyses of the eluted Zr(IV) (green), Ce(IV) (red), Th(IV) (purple), and Pu(IV) (light blue) species after electrospray ionization in positive detection mode.

Solution Stability and Polarity Trends for [M(IV)(3,4,3-LI(1,2-HOPO))] Complexes (M = Zr, Ce, Th, Pu). In general, f-block metal ions are considered to be hard Lewis acids, and, as such, they are commonly stabilized by oxygen-based ligands known to strongly bind transition metals, as demonstrated here with the 3,4,3-LI(1,2-HOPO) ligand.[16,18] In addition, the metal ions Zr^{4+}, Ce^{4+}, and Th^{4+} have often been hypothesized to behave in a similar manner to that of highly radioactive transuranic tetravalent ions and are commonly proposed for use as surrogates.[17,48−50] In particular, Ce^{4+} is considered to be an ideal nonradioactive replacement for Pu^{4+}, as a result of their nearly identical ionic radii.[51] While there is now a substantial amount of experimental evidence demonstrating that these

DOI: 10.1021/acs.inorgchem.5b00033
Inorg. Chem. 2015, 54, 3462−3468

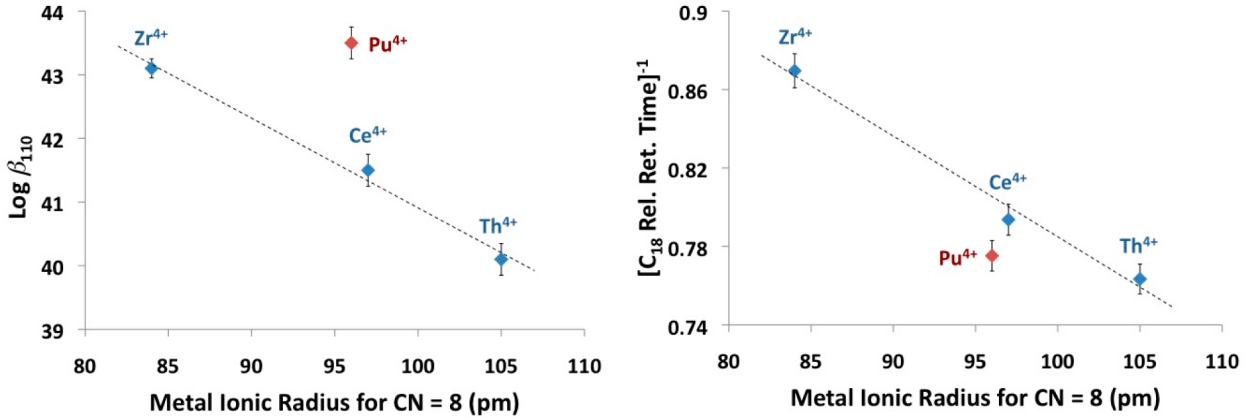

Figure 5. Stability constants (left) and polarity (right; measured as the inverse of chromatographic retention) for [M(IV))(3,4,3-LI(1,2-HOPO))] complexes (M = Zr, Ce, Th, and Pu (red)) as a function of metal ionic radii (CN = 8).

surrogates do not always properly mimic the behavior of 5f elements in the solid state, little data is available for comparisons in solution.[49] We have assembled here a series of solution data sets on 3,4,3-LI(1,2-HOPO) complexes of the four tetravalent metals Zr(IV), Ce(IV), Th(IV), and Pu(IV) that may add to the available body of data on their coordination similarities. Figure 5 depicts the trends in complex stability and overall polarity of the four metal complexes in solution as a function of the metal ionic radius for a coordination number of 8.[51] As expected, complex stability and polarity decrease over the series Zr(IV) > Ce(IV) > Th(IV) in an approximate linear fashion when plotted against the ionic radius, demonstrating the importance of the ionic radius in forming strong complexes with an octadentate ligand that bares four anionic charges when deprotonated. However, Pu(IV) seems to stand out, as it is found to form a complex considerably more stable but less polar than that of Ce(IV), despite the nearly identical size of both metal ions. On the basis of the position of the LMCT bands observed in the UV−vis spectra of the Ce(IV) (λ = 450 nm, ε = 1310 M^{-1} cm^{-1}) and Pu(IV) (λ = 390 nm, ε = 1070 M^{-1} cm^{-1}) complexes, the difference in energy levels for these transitions, ca. 4.0 eV, still indicates lower energy f orbitals for Ce than Pu, which would exclude an increase in covalent mixing due to near degeneracy of f orbitals that is sometimes observed in later actinide complexes formed with soft-donor ligands.[52] However, the Pu 5f orbitals may participate in some increased orbital mixing, which could explain the increased bond strength between the metal and ligand as well as the slightly decreased polarity, and the effect of electrostatic repulsion due to the presence of four 5f electrons in the Pu^{4+} species (with a $^5I_4$ ground term) should not be ignored. While the role of f-orbital bonding in Pu(IV) compared to that in Ce(IV) is largely speculative, these results are worth mentioning and certainly call to mind the finding of significant differences in coordination geometries in similar maltol complexes.[53] Further X-ray absorption spectroscopy and theory studies may be needed to unravel the significance of these findings.[52,54]

CONCLUSIONS

This work confirms that the hydroxypyridinonate octadentate ligand 3,4,3-LI(1,2-HOPO) forms highly stable complexes in aqueous solution with Zr(IV) and Pu(IV) ions, similar to what has been previously observed with Ce(IV) and Th(IV). Considering the known rapid metal complexation kinetics of HOPO functionalities, the facile insertion of a new conjugating linker through one of the amide groups of the spermine backbone, and its advanced preclinical characterization as a decorporation agent, 3,4,3-LI(1,2-HOPO) appears to be the most promising platform for the development of future ^{89}Zr-immuno-PET and ^{227}Th-α-immunotherapy agents. Future studies will focus on establishing synthetic procedures for conjugating mAbs and rapid and reproducible isotope labeling protocols for clinical settings as well as on exploring high-throughput synthetic methods for the preparation of new versatile HOPO-based ligands for heavy element coordination.

ASSOCIATED CONTENT

Supporting Information

Examples of fits for spectral data in metal competition batch titrations, metal stability constant determination as a function of proton concentration, and mass spectral data. This material is available free of charge via the Internet at http://pubs.acs.org.

AUTHOR INFORMATION

Corresponding Author

*E-mail: rjabergel@lbl.gov.

Notes

The authors declare no competing financial interest.

ACKNOWLEDGMENTS

We thank Prof. Kenneth Raymond, Dr. Linfeng Rao, Dr. Stefan Minasian, and Dr. Norman Edelstein for helpful discussions. This material is based on work supported by the U.S. Department of Energy, Office of Science Early Career Research Program and Office of Science, Office of Basic Energy Sciences, Chemical Sciences, Geosciences, and Biosciences Division at the Lawrence Berkeley National Laboratory under contract DE-AC02-05CH11231.

REFERENCES

(1) Deri, M. A.; Zeglis, B. M.; Francesconi, L. C.; Lewis, J. S. *Nucl. Med. Biol.* **2013**, *40*, 3−14.
(2) Zeglis, B. M.; Houghton, J. L.; Evans, M. J.; Viola-Villegas, N.; Lewis, J. S. *Inorg. Chem.* **2014**, *53*, 1880−1899.
(3) James, M. L.; Gambhir, S. S. *Physiol. Rev.* **2012**, *92*, 897−965.
(4) van Dongen, G. A. M. S.; Visser, G. W. M.; Hooge, M. N. L.-d.; De Vries, E. G.; Perk, L. R. *Oncology* **2007**, *12*, 1379−1389.
(5) Wadas, T. J.; Wong, E. H.; Weisman, G. R.; Anderson, C. J. *Chem. Rev.* **2010**, *110*, 2858−2902.

DOI: 10.1021/acs.inorgchem.5b00033
Inorg. Chem. 2015, 54, 3462−3468

(6) Price, E. W.; Orvig, C. *Chem. Soc. Rev.* **2014**, *43*, 260−290.
(7) Bottari, E.; Anderegg, G. *Helv. Chim. Acta* **1967**, *50*, 2349−&.
(8) Ilyukhin, A. B.; Davidovich, R. L.; Samsonova, I. N.; Teplukhina, L. V. *Crystallogr. Rep.* **2000**, *45*, 39−43.
(9) Parker, D.; Pulukkody, K.; Smith, F. C.; Batsanov, A.; Howard, J. A. K. *Dalton Trans.* **1994**, 689−693.
(10) Pozhidaev, A. I.; Poraikoshits, M. A.; Polynova, T. N. *J. Struct. Chem.* **1974**, *15*, 548−553.
(11) Meijs, W. E.; Haisma, H. J.; Van Der Schors, R.; Wijbrandts, R.; Van Den Oever, K.; Klok, R. P.; Pinedo, H. M.; Herscheid, J. D. M. *Nucl. Med. Biol.* **1996**, *23*, 439−448.
(12) Meijs, W. E.; Herscheid, J. D. M.; Haisma, H. J.; Pinedo, H. M. *Appl. Radiat. Isot.* **1992**, *43*, 1443−1447.
(13) Vosjan, M.; Perk, L. R.; Visser, G. W. M.; Budde, M.; Jurek, P.; Kiefer, G. E.; van Dongen, G. *Nat. Protoc.* **2010**, *5*, 739−743.
(14) Deri, M. A.; Ponnala, S.; Zeglis, B. M.; Pohl, G.; Dannenberg, J. J.; Lewis, J. S.; Francesconi, L. C. *J. Med. Chem.* **2014**, *57*, 4849−4860.
(15) Holland, J. P.; Divilov, V.; Bander, N. H.; Smith-Jones, P. M.; Larson, S. M.; Lewis, J. S. *J. Nucl. Med.* **2010**, *51*, 1293−1300.
(16) Brown, M. A.; Paulenova, A.; Gelis, A. V. *Inorg. Chem.* **2012**, *51*, 7741−7748.
(17) Natrajan, L. S.; Swinburne, A. N.; Andrews, M. B.; Randall, S.; Heath, S. L. *Coord. Chem. Rev.* **2014**, *266*−*267*, 171−193.
(18) Yusov, A. B.; Fedoseev, A. M. *Radiochemistry* **2013**, *55*, 360−365.
(19) Gorden, A. E. V.; Xu, J.; Raymond, K. N.; Durbin, P. W. *Chem. Rev.* **2003**, *103*, 4207−4282.
(20) Abergel, R. J.; Durbin, P. W.; Kullgren, B.; Ebbe, S. N.; Xu, J.; Chang, P. Y.; Bunin, D. I.; Blakely, E. A.; Bjornstad, K. A.; Rosen, C. J.; Shuh, D. K.; Raymond, K. N. *Health Phys.* **2010**, *99*, 401−407.
(21) Sturzbecher-Hoehne, M.; Kullgren, B.; Jarvis, E. E.; An, D. D.; Abergel, R. J. *Chem.—Eur. J.* **2014**, *20*, 9962−9968.
(22) Bunin, D. I.; Chang, P. Y.; Doppalapudi, R. S.; Riccio, E. S.; An, D. D.; Jarvis, E. E.; Kullgren, B.; Abergel, R. J. *Radiat. Res.* **2013**, *179*, 171−182.
(23) Chang, P. Y.; Bunin, D. I.; Gow, J.; Swezey, R.; Shinn, W.; Shuh, D. K.; Abergel, R. J. *J. Chromatogr. Sep. Tech.* **2011**, *4*, 196.
(24) Jarvis, E. E.; An, D. D.; Kullgren, B.; Abergel, R. J. *Drug Dev. Res.* **2012**, *73*, 281−289.
(25) Kullgren, B.; Jarvis, E. E.; An, D. D.; Abergel, R. J. *Toxicol. Mech. Methods.* **2013**, *21*, 18−26.
(26) Gorden, A. E. V.; Shuh, D. K.; Tiedemann, B. E. F.; Wilson, R. E.; Xu, J.; Raymond, K. N. *Chem.—Eur. J.* **2005**, *11*, 2842−2848.
(27) Deblonde, J. P.; Sturzbecher-Hoehne, M.; Abergel, R. J. *Inorg. Chem.* **2013**, *52*, 8805−8811.
(28) Welcher, F. J. *The Analytical Uses of Ethylenediamine Tetraacetic Acid*; D. van Nostrand Co.: Princeton, NJ, 1958.
(29) Gans, P.; Sabatini, A.; Vacca, A. *Talanta* **1996**, *43*, 1739−1753.
(30) Gans, P.; Sabatini, A.; Vacca, A. *HypSpec*; Protonic Software: Leeds, UK, 2008.
(31) Abergel, R. J.; D'Aleo, A.; Ng Pak Leung, C.; Shuh, D. K.; Raymond, K. N. *Inorg. Chem.* **2009**, *48*, 10868−10870.
(32) Sturzbecher-Hoehne, M.; Ng Pak Leung, C.; D'Aleo, A.; Kullgren, B.; Prigent, A. L.; Shuh, D. K.; Raymond, K. N.; Abergel, R. J. *Dalton Trans.* **2011**, *40*, 8340−8346.
(33) Martell, A. E.; Smith, R. M.; Motekaitis, R. J. *NIST Critically Selected Stability Constants of Metal Complexes*, version 8.0; NIST: Gaithersburg, MD, 2004.
(34) Alderighi, L.; Gans, P.; Ienco, A.; Peters, D.; Sabatini, A.; Vacca, A. *Coord. Chem. Rev.* **1999**, *184*, 311−318.
(35) Alderighi, L.; Gans, P.; Ienco, A.; Peters, D.; Sabatini, A.; Vacca, A. *HYSS*; Protonic Software: Leeds, UK, 2009.
(36) Hu, Y.-J.; Knope, K. E.; Skanthakumar, S.; Kanatzidis, M. G.; Mitchell, J. F.; Soderholm, L. *J. Am. Chem. Soc.* **2013**, *135*, 14240−14248.
(37) Kalaji, A.; Soderholm, L. *Inorg. Chem.* **2014**, *53*, 11252−11260.
(38) Ruther, R. E.; Baker, B. M.; Son, J.-H.; Casey, W. H.; Nyman, M. *Inorg. Chem.* **2014**, *53*, 4234−4242.
(39) Rand, M. H.; Fuger, J.; Grenthe, I.; Neck, V.; Rai, D. In *Chemical Thermodynamics*; OECD Nuclear Energy Agency: Paris, 2008; Vol. *11*.
(40) Durbin, P. W. *Health Phys.* **2008**, *95*, 465−492.
(41) Holland, J. P.; Sheh, Y.; Lewis, J. S. *Nucl. Med. Biol.* **2009**, *36*, 729−739.
(42) Zhang, Y.; Hong, H.; Cai, W. *Curr. Radiopharm.* **2011**, *4*, 131−139.
(43) Sturzbecher-Hoehne, M.; Deblonde, J. P.; Abergel, R. J. *Radiochim. Acta* **2013**, *101*, 359−366.
(44) Whisenhunt, D. W.; Neu, M. P.; Hou, Z. G.; Xu, J.; Hoffman, D. C.; Raymond, K. N. *Inorg. Chem.* **1996**, *35*, 4128−4136.
(45) Larsen, R.; Bruland, O. Patent WO2004091668A1, 2004.
(46) Pham, T. A.; Xu, J.; Raymond, K. N. *J. Am. Chem. Soc.* **2014**, *136*, 9106−9115.
(47) Ruegg, C. L.; Anderson-Berg, W. T.; Brechbiel, M. W.; Mirzadeh, S.; Gansow, O. A.; Strand, M. *Cancer Res.* **1990**, *50*, 4221−4226.
(48) Behrle, A. C.; Levin, J. R.; Kim, J. E.; Drewett, J. M.; Barnes, C. L.; Schelter, E. J.; Walensky, J. R. *Dalton Trans.* **2014**, *44*, 2693−2702.
(49) Diwu, J.; Nelson, A. G. D.; Albrecht-Schmitt, T. E. *Comments Inorg. Chem.* **2010**, *31*, 46−62.
(50) Diwu, J.; Wang, S.; Liao, Z.; Burns, P. C.; Albrecht-Schmitt, T. E. *Inorg. Chem.* **2010**, *49*, 10074−10080.
(51) Shannon, R. D. *Acta Crystallogr.* **1976**, *A32*, 751−767.
(52) Neidig, M. L.; Clark, D. L.; Martin, R. L. *Coord. Chem. Rev.* **2013**, *257*, 394−406.
(53) Szigethy, G.; Xu, J.; Gorden, A. E. V.; Teat, S. J.; Shuh, D. K.; Raymond, K. N. *Eur. J. Inorg. Chem.* **2008**, 2143−2147.
(54) Minasian, S. G.; Keith, J. M.; Batista, E. R.; NBoland, K. S.; Clark, D. L.; Conradson, S. D.; Kozimor, S. A.; Martin, R. L.; Schwarz, D. E.; Shuh, D. K.; Wagner, G. L.; Wilkerson, M. P.; Wolfsberg, L. E.; Yang, P. *J. Am. Chem. Soc.* **2012**, *134*, 5586−8897.
(55) Anderegg, G.; Arnaud-Neu, F.; Delgado, R.; Felcman, J.; Popov, K. *Pure Appl. Chem.* **2005**, *77*, 1445−1495.

DOI: 10.1021/acs.inorgchem.5b00033
Inorg. Chem. 2015, 54, 3462−3468